Arabian Journal of Chemistry (2023) **16**, 104876

King Saud University

Arabian Journal of Chemistry

www.ksu.edu.sa
www.sciencedirect.com

ORIGINAL ARTICLE

Oil-in-water strategy coating Curcumin-*nido*-Carborane fluorescent complex with acrylic resins for cell imaging

Chen Lu [a,1], **Zhendong Yao** [b,1], **Jiankang Feng** [c], **Boneng Mao** [b,*], **Guofan Jin** [c,*]

[a] *Pukou Branch of Jiangsu People's hospital, Nanjing Pukou District Central Hospital, Nanjing 210000, PR China*
[b] *Department of Gastroenterology, The Affiliated Yixing Hospital of Jiangsu University, Yixing 214200, PR China*
[c] *School of Pharmacy, Jiangsu University, Zhenjiang 212013, PR China*

Received 22 September 2022; accepted 29 March 2023
Available online 5 April 2023

KEYWORDS

Curcumin;
Carborone;
Oil-in-water;
Acrylic resin;
Cell imaging

Abstract Using curcumin and carborane as raw materials, four different kinds of curcumin fluorescent complexes RL-100-Curcumin (RL-100-Cur), RS-100-Curcumin (RS-100-Cur), RL-100-Curcumin -Carborane (RL-100-Cur-B) and RS-100-Curcumin-Carborane (RS-100-Cur-B) were prepared by one-pot method, which solved the shortcomings of curcumin's poor solubility and improved the biocompatibility of curcumin-carboranes. The prepared fluorescent complexes were characterized by infrared spectroscopy, and the characteristic peaks at 1634 cm^{-1} (aromatic), 1732 cm^{-1} (carbonyl) and 2568 cm^{-1} (boron) were confirmed. The coating of curcumin-carborane into nano-spheres by acrylic resin carrier can be observed by transmission electron microscope. Acrylic resins RL-100 and RS-100 are zwitteric ionic polychloride polymer materials, which can be firmly combined with polar or ionic molecules in the form of hydrogen or ionic bonds to form regular nanoparticle. Through in vitro tumor cell imaging, it was observed that the four kinds of curcumin fluorescent complexes had good biocompatibility and accurately entered into tumor cells, indicating that the four compounds had certain selectivity. This design not only solves the problem of curcumin-carborane bioavailability but also has a certain visual fluorescence targeting effect. In particular, the properties of RS-100-Cur-B are particularly obvious.

1. Introduction

Curcumin is a phenolic pigment extracted from turmeric, which has important medicinal value(Ali et al., 2020, Liu et al., 2022, Liu 2022, Bar-Sela et al., 2010, Bhawana et al., 2011). Studies have found that the main pharmacological effects of curcumin include antioxidant, anti-inflammatory, anticoagulant, lipid-lowering, anti-atherosclerosis, anti-aging, free radical elimination and tumor growth inhibition (Calabrese et al., 2012, Hu et al., 2022, Lupina et al., 2023, Cui et al., 2021). Curcumin can inhibit the proliferation, invasion and metastasis of tumor cells, which further explains the biological value

* Corresponding authors.
E-mail addresses: staff562@yxph.com, organiboron@ujs.edu.cn (G. Jin).
[1] These authors have contributed equally to this work.
Peer review under responsibility of King Saud University.

Production and hosting by Elsevier

https://doi.org/10.1016/j.arabjc.2023.104876
1878-5352

of curcumin in tumor therapy. At the same time, curcumin has also become the focus of anti-tumor research at home and abroad, involving more and more extensive research fields. The antitumor mechanism of curcumin is very complex and varied, mainly including the following three points: 1) inducing apoptosis of tumor cells; 2) stasis of tumor cell cycle; 3) Inhibit the proliferation and metastasis of tumor cells and the angiogenesis of tumor tissues.

As a new tumor targeting drug, carborane ($C_2H_{12}B_{10}$) has a very high cure rate and survival rate for refractory tumor diseases(Metawea et al., 2021, Mehany et al., 2023, Duceac et al., 2023, Fu et al., 2021). Carborane has a regular dodecahedral spatial conformation similar to the miniaturized C60 structure and is similar in volume size to the benzene ring. According to the relative positions of the two carbon atoms, they can be divided into *ortho*-carborane, *meta*-carborane and *para*-carborane. In terms of chemical structure, carborane has a special large steric hindrance skeleton, so it has a strong hydrophobicity. Therefore, the chemical structure modification of carborane can not only play a stable role, but also improve the solubility and biocompatibility of carborane in aqueous solution. However, because curcumin and carborane are insoluble in water, they are difficult to be absorbed by the human body through the intestinal wall, so the biological functional role of curcumin and carborane is not fully utilized(Shao et al., 2022, Dai et al., 2022, Gutierrez et al., 2017). In addition, its poor stability and other defects greatly limit its application in the medical field(Wang et al., 2021, Kharat et al., 2018). Their water-soluble research has the following types, such as solution or emulsion dosage form, changing its chemical structure, preparing into nanoparticles and so on, among which the nano preparation has become a hot research field(Kocaadam et al., 2017, Mirzaei et al., 2018, Mirzaei et al., 2017, Olusanya et al., 2019).

Acrylic resin as a good pharmaceutical coating materials. They are relatively stable in the human stomach environment, and are less affected by digestive enzymes. They will swell in the human body fluid environment and form multiple channels, but they will not be absorbed by the human body, not to be metabolized by the human liver(Deng et al., 2021, Pillai et al., 2014, Pushpakumari et al., 2015, Rasheed et al., 2017). A inclusion compound is a unique form of complex in which a drug molecule is wholly or partially enclosed in the molecular cavity of another substance. The coating process of inclusion complex is a physical process, which does not involve the breaking of the old chemical bond and the formation of the new chemical bond. It just changes the state of the substance, and does not produce new substances, so it is not a chemical reaction. Therefore, the stability of the inclusion complex is mainly dependent on the interaction forces between the wrapping and the covering, including van der waals forces, hydrogen bonds formed, and so on. The coating process of clathrate is a dynamic process, rather than a static one. While the coated substances continue to enter the cavity, the coated substances also continue to flow out of the cavity.(Salehi et al., 2019, Xu et al., 2021, Stanic et al., 2017, Wang et al., 2021, Marinho et al., 2023).

A series of problems such as curcumin-carborane insolubility were summarized, and the concept of acrylic resin coating was further considered and designed. Firstly, the structures of curcumin and carborane were modified, and two carbonyl groups were introduced into the fluorophores, and the carborane potassium salt was introduced again without changing its biological activity to further resolve the solubility problem. Secondly, the nano-form was prepared by acrylic resin coating. Finally, the biocompatibility and selectivity were observed by tumor cell imaging.

2. Experimental section

2.1. Chemistry

2.1.1. General experimental conditions

All solvents and reagents were purchased commercially and used without further purification. The reagents used are curcumin (98%, RG), Acrylic resin RL-100 (RG), Acrylic resin RS-100 (RG), HeLa (Product code: CTCC-001–0006/HTX1651) and carborane (98%, RG), which were purchased through commercial channels such as Titan Technologies. The Biological consumables used: DMEM/HIGH GLUCOSE medium (Product code: AF29498406), RPMI 1640 medium (Product code: 70080192), Pancreatic enzyme cell digestive fluid (Product code: 70080900) and PBS (Product code: PBSGNM20012), which were purchased through commercial channels such as Hyclone, biosharp, Bioshop and genomcell.bio. All glassware were oven-dried and kept in a desiccator before use. Analysis of TLC results at 254 nm and 360 nm wavelengths under UV lamps.

2.1.2. General procedure for the preparation of product

Take a 25 mL round-bottom flask, the acrylic resin RL-100 (70 mg) and curcumin (70 mg) were dissolve in EtOH (3 mL), and then at the room temperature stirred for 8hrs. The EtOH was concentrated to afford 130 mg of L100-Cur (Scheme 1).

The fluorescent complexes RS-100- Cur, RL-100-Cur-B and RS-100-Cur-B were obtained by the same method.

2.2. Spectroscopic properties

2.2.1. UV spectrum

Ultraviolet–visible (UV–vis) spectra were recorded on a UV-2550 spectrophotometer using a 1 cm path length quartz cuvette. The 10 mg fluorescent complex was dissolved in methylene chloride (MC), ethyl acetate (EA), dimethyl sulfoxide (DMSO) and tetrahydrofuran (THF), respectively, to prepare the required optimal concentration gradient for future use. Spectral tests of solutions with different concentrations were prepared according to needs and data were recorded. The UV–Vis wavelength range is 400–700 nm. The fluorescence of the complex was obtained at the optical path of 10 mm and the excitation wavelength of 450 nm, and the wavelength range of the recorded emission was 400–800 nm.

2.2.2. Fluorescence emission spectrum

Fluorescence Spectra were performed on Shimadzu RF-5301PCS Spectro fluorophotometer at room temperature. The four fluorescent complex were dissolved in MC and formulated into a series of concentrations and then the fluorescence spectra were tested in EA, DMSO and THF solutions. Set the excitation wavelength as the corresponding maximum absorption wavelength in ultraviolet. The corresponding fluorescence emission spectrum was obtained.

2.2.3. IR spectrum

Grind the dried sample and potassium bromide into fine powder in agate mortar under an infrared lamp. Take the fine powder of potassium bromide into the tablet pressing die, make a transparent sheet on the tablet pressing machine, put the ingot into the sample chamber of the spectrometer to obtain the blank infrared spectrum, move the mixture of four samples and potassium bromide into the tablet pressing die to press the tablet, and scan the spectrum to obtain the infrared spectrum.

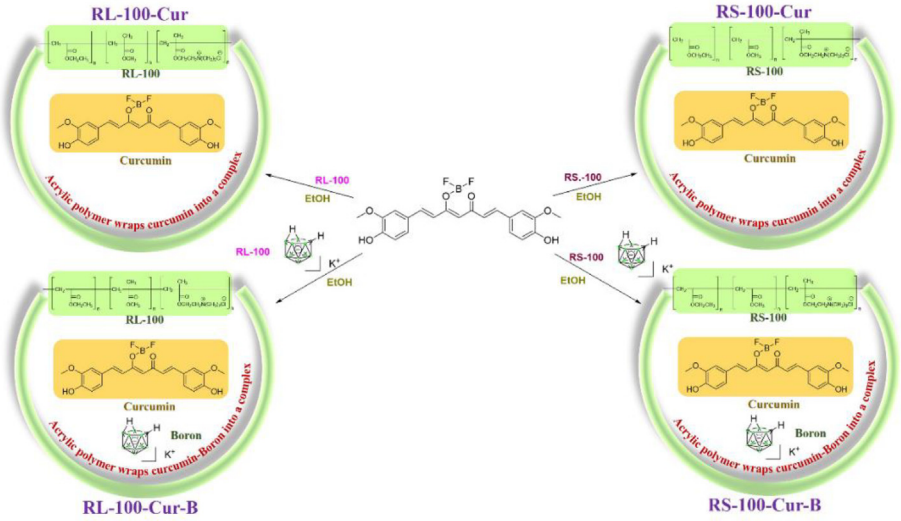

Scheme 1 Synthesis route of curcumin fluorescence complexes.

2.3. Biological

2.3.1. Cellular uptake and localization by transmission electron microscope

A thin supporting film is adhered on the copper net in advance, and a proper amount of powder and tetrahydrofuran are added to the small beaker respectively, and ultrasonic oscillation is carried out for 10–30 min. After 3–5 min, the uniform mixed liquid of powder and tetrahydrofuran is sucked by a glass capillary tube, and then 2–3 drops of the mixed liquid are dropped onto the copper net and dried. Wait for more than 15 min to volatilize tetrahydrofuran as much as possible. Finally, put the sample on the sample table and insert it into the electron microscope for observation.

2.3.2. Cell imaging

HeLa cells at logarithmic growth stage were treated with trypsin, inoculated in 96 well plates with circular plates, placed in 5% CO_2 incubator, cultured at 37 °C for 24 h, and adhered to the wall. In DMSO, the prepared resin RL-100-Cur, RS-100-Cur, RL-100-Cur-B and RS-100-Cur-B stock solutions (5 mg/ml) were respectively diluted with DMSO to prepare solutions with appropriate concentrations. The cells in the original culture medium were deleted in each and replaced by cells containing 5 μg/ml of different media for 36 h. After that, they were discarded in PBS, washed twice, and then fixed with paraformaldehyde for 20 min. The solution eliminated the repair solution was incubated with PBS and washed twice, the DAPI dark room was incubated for 20 min, the staining solution was discarded, and the PBS was washed twice. After the anti-fluorescence inactivated scaffold treatment, the cell fluorescence image was obtained on the fluorescence microscope.

3. Results and discussion

Acrylic resin can be divided into many types because of its different structure, molecular weight and water solubility. In order to increase its solubility, we selected two acrylic resins RL-100 and RS-100 to solve the solubility of curcumin-carborane itself. It can be seen from Scheme 1 that the structural characteristics of two different types of acrylic resins are all with quaternary ammonium salt groups, while the carborane is treated with potassium hydroxide to obtain potassium salt, which increases the ionic binding ability and water solubility of acrylic resins. These functional groups can form hydrogen bonds with hydrogen and hydroxide ions in the water environment, which can greatly increase the solubility, and facilitate the coating of lipid-soluble curcumin-carborane into the water environment.

From the four infrared spectra, it can be observed that RL-100-Cur-B and RS-100-Cur-B (Fig. 1) have a strong absorption peaks in the range of 2568 cm^{-1}, which is the characteristic peak of the boron spectrum of carborane. In contrast, RL-100-Cur and RS-100-Cur do not have such absorption peaks, mainly because there are no carborane molecules coated in these two fluorescent complexes. The strong absorption peaks in the range of 1732 cm^{-1} is the characteristic absorption peak of the two carbonyl groups of curcumin, while the subsequent absorption peak in the range of 1634–1455 cm^{-1} belongs to the aromatic absorption peak. And the smooth absorption peaks at 3441 cm-1 at the far left are characteristic peaks of hydroxyl and amine groups in acrylic polymer (Fig. 2).

The MC, EA, DMSO and THF were used as solvents for UV spectrum analysis. The results show that the UV absorption spectra of RS-100-Cur and RL-100-Cur fluorescent complexes have the same double peaks in the range of 430 ~ 470 nm, respectively, and the maximum absorption wavelength is in the range of 460 ~ 470 nm. This is because curcumin has an absorption peak at 200–300 nm and 410–450 nm respectively, and the maximum absorption peak in the visible range is at 400 nm, while there is almost no absorption at 500–800 nm. The results showed that curcumin could not be activated in the range of 500–800 nm, but could be activated in the range of 200–300 nm and 410–450 nm.The UV absorption spectra of RS-100-Cur-B and RL-100-Cur-B fluorescent complexes showed similar multiple trailing peaks, and the maximum absorption wavelength was in the range of 330–360 nm, and the absorption intensity

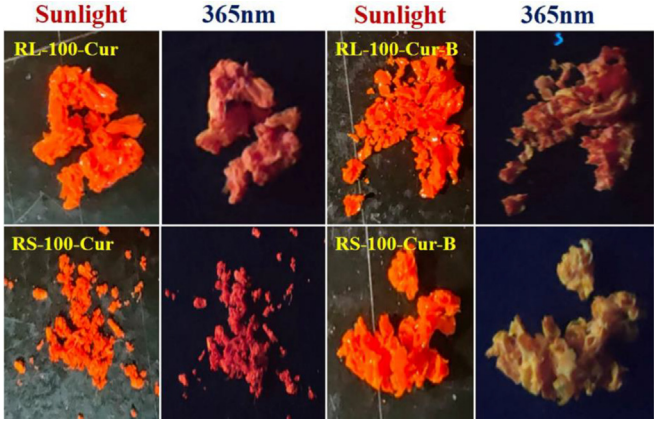

Fig. 1 Sunlight and 365 nm images of four curcumin fluorescence complexes.

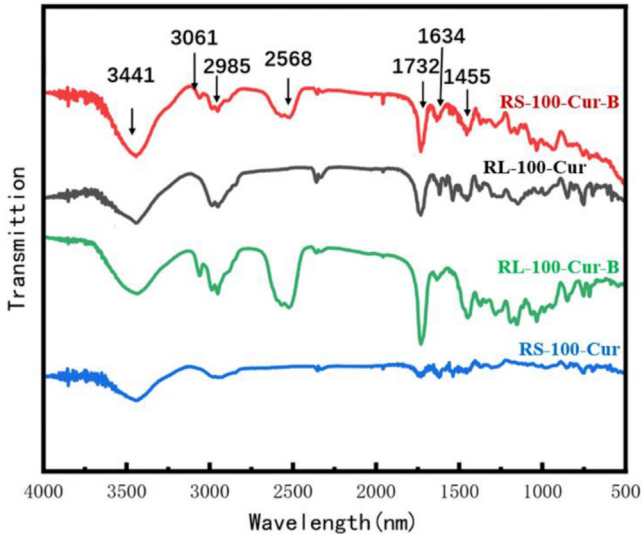

Fig. 2 Infrared spectrum of curcumin fluorescence complexes.

also increased with the increase of concentration, but the wavelength decreases. This is due to the interference of carborane which affects the absorption peak of curcumin and causes the instability phenomenon such as multiple peaks, resulting in the gradual weakening of its wavelength range. (Fig. 3 and Table 1).

Similarly, the fluorescence emission spectra of the four fluorescent complexes were tested in MC, EA, DMSO and THF. The fluorescence emission spectra of RS-100-Cur and RL-100-Cur fluorescent complexes are in the range of $486 \sim 512$ nm, and the emission intensity is basically in the range of $10000 \sim 4000$. The fluorescence emission spectra of RS-100-Cur-B and RL-100-Cur-B fluorescent complexes show weak emission intensity in the range of $1000 \sim 400$. On the one hand, it is due to the solubility difference of different solvents, on the other hand, carborane interference leads to their emission intensity difference of more than 10 times.

In addition, the relative photoluminescence fluorescence quantum yield Φf of four fluorescent complexes was measured and calculated using Rhodamine B (Φf = 0.5) in buffer solution and used as a reference for target compounds. The fluorescence quantum yields of RS-100-cur-B and RL-100-cur-B were 0.038 and 0.051 respectively, both of which were lower than that of RS-100-Cur and RL-100-Cur. This is because the addition of carborane makes the steric hindrance of the whole increase, and the degree of conjugation of the molecule decreases, leading to the decrease of quantum yield. This also proves that the phenomena in the UV absorption spectrum described above are consistent. (Fig. 4 and Table 1).

In order to observe the internal morphology more directly, four kinds of fluorescent complex were tested by transmission electron microscopy. As can be seen from the picture, these fluorescent complexes have form of nanoparticles and are uniformly dispersed in the system. These four sets of images have very unique features. For example, RL-100-Cur and RS-100-urR nanoparticles are fluffed together like clusters of cotton, while RL-100-Cur-B and RS-100-Cur-B are very obvious solid nanoparticles. This is because the former is acrylic resin coated curcumin, while the latter is acrylic resin coated curcumin and carborane. The carborane itself has the three-dimensional structure of dodecahedron in the shape of a sphere. It can be clearly observed by the TEM that the carborane particles are coated with acrylic resin and tightly aggregated together. These images show that the acrylic resin tightly coats the two materials to form nanoparticles (Fig. 5).

The selectivity, affinity and biocompatibility of the four fluorescent complexes in tumor cells were studied by cell imaging according to their structural characteristics. HeLa cell staining under the laser confocal microscope can be clearly seen under the fluorescence microscope.

As shown in Fig. 6, bright field, DAPI, green channel, red channel and merge imaging are provided. The selectivity, affinity and biocompatibility of the four fluorescent complexes with HeLa cells were improved compared with the two control groups. However, the cell imaging effect of RL-100-Cur-B and RS-100-Cur-B is more obvious than that of RL-100-Cur and RS-100-Cur. This is because the coating carborane potassium salt increases the affinity with HeLa cells, leading to different effects between the two groups. Moreover, carborane itself has a very good selective effect on tumor cells, which further increases the targeting effect. In particular, the effect of RS-100-Cur-B is significant, and it was observed that the fluorescent complex almost surrounded or entered the tumor cells.

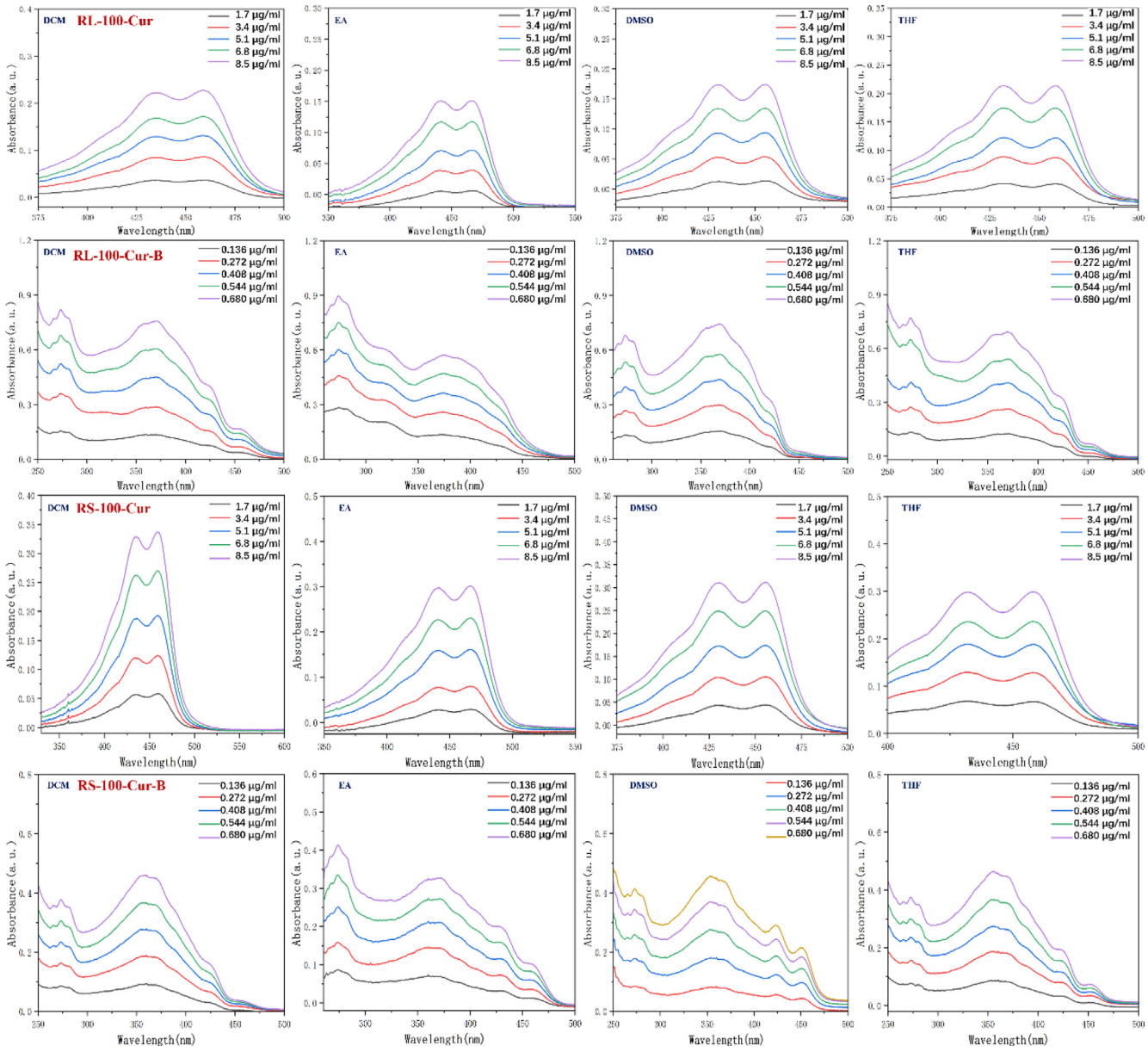

Fig. 3 UV absorption spectrum of fluorescent complexes RL-100-Cur, RS-100-Cur, RL-100-Cur-B and RS-100-Cur-B in different solvents.

Table 1 Absorption and emission spectra data in different solutions of four fluorescent complexes.

Fluorescent Complex	Items	Solvents				Φ_f[a]
		DCM	EA	THF	DMSO	
RS-100-Cur	λ_{abc}/nm	459	464	458	462	0.312
	λ_{em}/nm	510	512	485	484	
RL-100-Cur	λ_{abc}/nm	460	469	458	459	0.263
	λ_{em}/nm	512	512	487	485	
RS-100-Cur-B	λ_{abc}/nm	458	458	452	461	0.038
	λ_{em}/nm	470	480	482	475	
RL-100-Cur-B	λ_{abc}/nm	458	434	430	454	0.051
	λ_{em}/nm	470	472	465	474	

[a] photoluminescence quantum yield estimated relative to rhodamine B as the standard (Uf = 0.5 in ethanol).

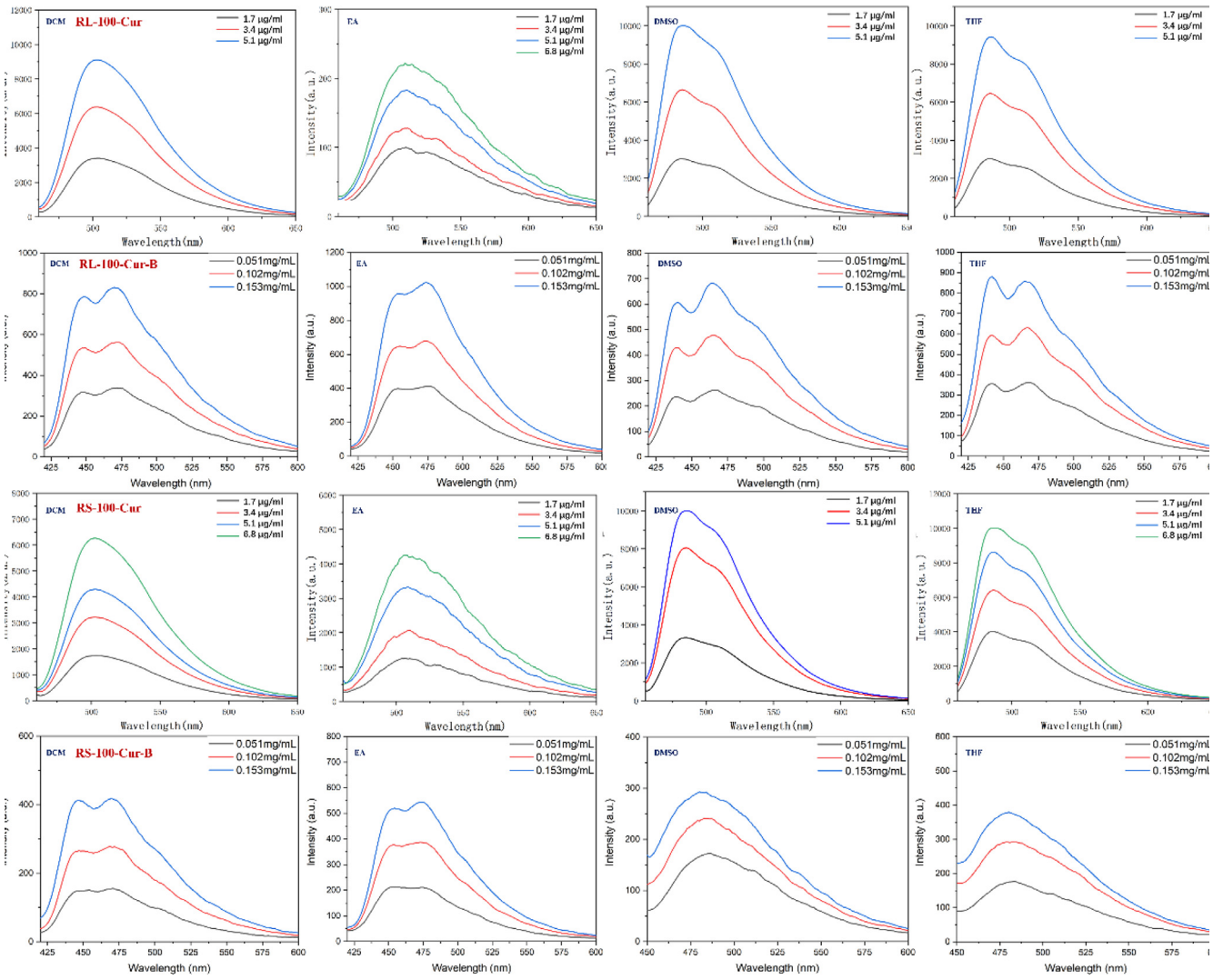

Fig. 4 Fluorescence emission spectrum of fluorescent complexes RL-100-Cur, RS-100-Cur, RL-100-Cur-B and RS-100-Cur-B in different solvents.

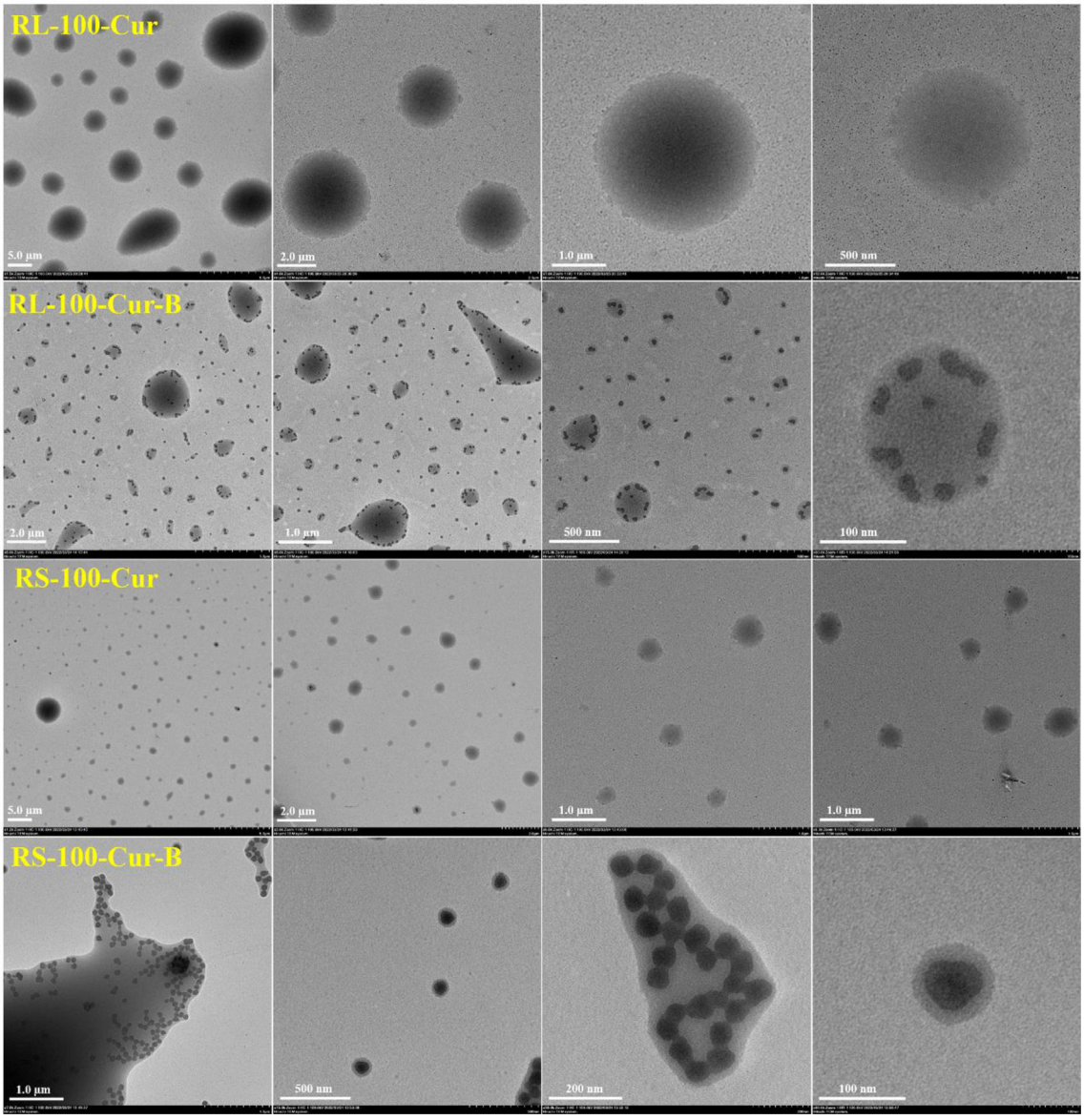

Fig. 5 Transmission electron microscope images of fluorescent complexes RL-100-Cur, RS-100-Cur, RL-100-Cur-B and RS-100-Cur-B.

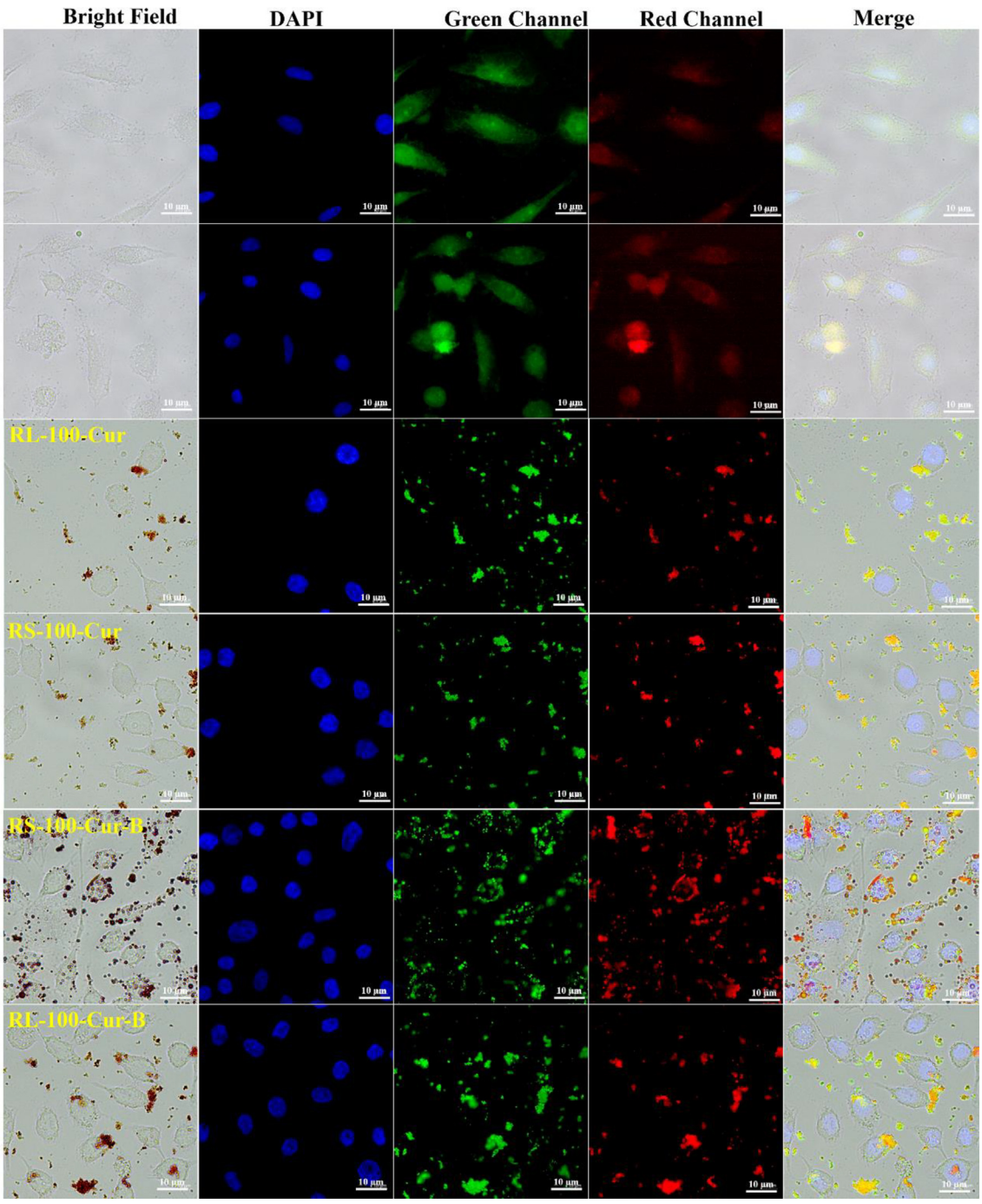

Fig. 6 Cellular imaging of RL-100-Cur, RS-100-Cur, RL-100-Cur-B and RS-100-Cur-B.

4. Conclusion

Through the research of the subject, fat-soluble curcumin and carborane are coated with acrylic resin to achieve "oil-in-water" effect and increase its compatibility with tumor cells. This design shows good application potential, and novel fluorescent composite drugs are prepared by an outside-in approach combining pharmaceutical excipients and zwitterion technology, which not only solves the problem of incompatibility, but also enables curcumin-carborane fluorescent complex are driven into tumor cells by aggregation-induced dynamic self-assembly. These relevant data can provide theoretical feasibility basis for subsequent research on curcumin-carborane fluorescent complexes.

Declaration of Competing Interest

The authors declare that they have no known competing financial interests or personal relationships that could have appeared to influence the work reported in this paper.

Acknowledgement

This study was supported financially by the scientific research foundation of Jiangsu University (Grant No. 17JDG002), and the cell experimental data provided by Pukou Branch of

Jiangsu People's hospital and the Affiliated Yixing Hospital of Jiangsu University.

References

Ali, F., Hosmane, N.S., Zhu, Y., et al, 2020. Boron chemistry for medical applications. Molecules 25, 828. https://doi.org/10.3390/molecules25040828.

Bar-Sela, G., Epelbaum, R., Schaffer, M., et al, 2010. Curcumin as an anti-cancer agent: review of the gap between basic and clinical applications. Curr. Med. Chem. 17, 190–197. https://doi.org/10.2174/092986710790149738.

Bhawana, R. K. Basniwal, H. S. Buttar, et al., 2011. Curcumin Nanoparticles: Preparation, Characterization, and Antimicrobial Study. J. Agric. Food Chem. 59, 2056-2061. 10.1021/jf104402t

Calabrese, G., Nesnas, J.J., Barbu, E., et al, 2012. The formulation of polyhedral boranes for the boron neutron capture therapy of cancer. Drug Discov. Today 17, 153–159. https://doi.org/10.1016/j.drudis.2011.09.014.

Cui, M.-h., E.-h. Fu, Z.-h. Lin, et al., 2021. Research progress of pharmacological functions on tumor suppression by curcumin. Zhongguo Linchuang Yaolixue Zazhi. 37, 92. 10.13699/j.cnki.1001-6821.2021.02.022.

Dai D., He., Feng J., Lian G., Jin, G. F, et al., 2022. Water-soluble BODIPY-nido-carborane nanoparticles applied to biocompatibility tumor cell imaging. Photochemical & Photobiological Sciences. 21, 185-194. 10.1007/s43630-021-00148-1

Deng P., Xiao F., Jin G. F, et al., 2021. A Novel BODIPY Quaternary Ammonium Salt-Based Fluorescent Probe: Synthesis, Physical Properties, and Live-Cell Imaging. Frontiers in chemistry. 9, 650006. 10.3389/fchem.2021.650006

Fu, Y.-S., Chen, T.-H., Weng, L., et al, 2021. Pharmacological properties and underlying mechanisms of curcumin and prospects in medicinal potential. Biomed. Pharmacother. 141,. https://doi.org/10.1016/j.biopha.2021.111888 111888.

Gutierrez, J. K. T., G. C. Zanatta, A. L. M. Ortega, et al., 2017. Encapsulation of curcumin in polymeric nanoparticles for antimicrobial photodynamic therapy. PLoS One. 12, e0187418/0187411. 10.1371/journal.pone.0187418.

Hu, J., Liu, Y., Hu, K., Lian, G., Zhou, M., Jin, G.F., et al, 2022. Simple and practical, highly sensitive and responsive recognition of cysteine: design, synthesis and mechanism study of a novel curcumin fluorescent probe. Arab. J. Chem. 15,. https://doi.org/10.1016/j.arabjc.2022.104087 104087.

Kharat, M., Zhang, G., McClements, D.J., 2018. Stability of curcumin in oil-in-water emulsions: impact of emulsifier type and concentration on chemical degradation. Food Res. Int. 111, 178–186. https://doi.org/10.1016/j.foodres.2018.05.021.

Kocaadam, B., Sanlier, N., 2017. Curcumin, an active component of turmeric (Curcuma longa), and its effects on health. Crit. Rev. Food Sci. Nutr. 57, 2889–2895. https://doi.org/10.1080/10408398.2015.1077195.

Liu, Y., Hu, K., Lian, G., Zhou, M., Jin, G.F., et al, 2022. Bioactivity and cell imaging of antitumor fluorescent agents (Curcumin Derivatives) coated by two-way embedded cyclodextrin strategy. Chem. Biodivers. 19, e202200644.

Liu, Y., Hu, K., Lian, G., Zhou, M., Jin, G.F., et al, 2022. Curcumin copolymerized drugs mediated by enteric-coated polymers: their design, synthesis and biocompatibility cell imaging studies. Eur. Polym. J. 180,. https://doi.org/10.1016/j.eurpolymj.2022.111606 111606.

Lupina, K., Kowalczyk, D., Lis, M., Basiura-Cembala, Mo, et al., 2023. Antioxidant polysaccharide/gelatin blend films loaded with curcumin - A comparative study. International Journal of Biological Macromolecules. Ahead of Print. 10.1016/j.ijbiomac.2023.123945

Marinho, J. P. N., Edesia M. B. d, et al., 2023. Nanostructured system based on hydroxyapatite and curcumin: A promising candidate for osteosarcoma therapy. Ceramics International. Ahead of Print. 10.1016/j.ceramint.2023.03.115

Mehany, A. B. M., Farrag, I. M., Shaaban, S., Abdelhady, A. A, et al., 2023. Curcumin and vitamin C improve immunity of kidney via gene expression against diethyl nitrosamine induced nephrotoxicity in rats:In vivo and molecular docking studies. Heliyon. Ahead of Print. 10.1016/j.heliyon.2023.e14126.

Mirzaei, H., Shakeri, A., Rashidi, B., et al, 2017. Phytosomal curcumin: a review of pharmacokinetic, experimental and clinical studies. Biomed. Pharmacother. 85, 102–112. https://doi.org/10.1016/j.biopha.2016.11.098.

Mirzaei, H., Masoudifar, A., Sahebkar, A., et al, 2018. MicroRNA: a novel target of curcumin in cancer therapy. J. Cell. Physiol. 233, 3004–3015. https://doi.org/10.1002/jcp.26055.

Olusanya, T.O.B., Calabrese, G., Fatouros, D.G., et al, 2019. Liposome formulations of o-carborane for the boron neutron capture therapy of cancer. Biophys. Chem. 247, 25–33. https://doi.org/10.1016/j.bpc.2019.01.003.

Pillai, J.J., Thulasidasan, A.K.T., Anto, R.J., et al, 2014. Folic acid conjugated cross-linked acrylic polymer (FA-CLAP) hydrogel for site specific delivery of hydrophobic drugs to cancer cells. J. Nanobiotechnol. 12, 25/21. https://doi.org/10.1186/1477-3155-12-25.

Pushpakumari, K.N., Varghese, N., Kottol, K., 2015. Enhancing the absorption of curcuminoids from formulated turmeric extracts. Int. J. Pharm. Sci. Res. 6, 2468–2476. https://doi.org/10.13040/ijpsr.0975-8232.6(6).2468-76.

Rasheed, A., P. R. Yalavarthi, H. Cheramparambil, et al., 2017. Synthesis and Pharmacological Evaluation of Acrylate-Based Gastrosparing NSAID Prodrugs. Arch. Pharm. (Weinheim, Ger.). 350, n/a. 10.1002/ardp.201600325

Salehi, B., Stojanovic-Radic, Z., Matejic, J., et al, 2019. The therapeutic potential of curcumin: a review of clinical trials. Eur. J. Med. Chem. 163, 527–545. https://doi.org/10.1016/j.ejmech.2018.12.016.

Shao, T., Wang, Y., Hu, K., Lian, G., Jin, G.F., et al, 2022. Nitrogen-boron eight-ring rigid cis/trans BODIPY-pyrimidine isomers for in vivo and in vitro fluorescence target recognition and evaluation of inhibitory activity. Dyes and Pigment. 201,. https://doi.org/10.1016/j.dyepig.2022.110204 110204.

Stanic, Z., 2017. Curcumin, a compound from natural sources, a true scientific challenge - a review. Plant Foods Hum. Nutr. 72, 1–12. https://doi.org/10.1007/s11130-016-0590-1.

Wang Y., Xiao F., Shao T., Hu K., Lian G., Feng J., Chen H., Jin G. F, et al., 2021. A multiple acetal chalcone-BODIPY-based fluorescence: synthesis, physical property, and biological studies. Analytical and bioanalytical chemistry. 413, 2529-2541. 10.1007/s00216-021-03208-8

Wang, Y., Sun, R., Xu, X., et al, 2021. Structural interplay between curcumin and soy protein to improve the water-solubility and stability of curcumin. Int. J. Biol. Macromol. 193, 1471–1480. https://doi.org/10.1016/j.ijbiomac.2021.10.210.

Xu, C., Shao, T., Shao, S., Jin, G.F., et al, 2021. High activity, high selectivity and high biocompatibility BODIPY-pyrimidine derivatives for fluorescence target recognition and evaluation of inhibitory activity. Bioorg. Chem. 114,. https://doi.org/10.1016/j.bioorg.2021.105121 105121.

Further reading

Duceac, I.A., Verestiuc, L., Dimitriu, C.D., et al, 2020. Design and preparation of new multifunctional hydrogels based on chitosan/acrylic polymers for drug delivery and wound dressing applications. Polymers (Basel Switz.) 12, 1473. https://doi.org/10.3390/polym12071473.

Metawea, M. R., Abdelrazek, H. M. A., El-Hak, H. N. Gad., Moghazee, M. M., Marie, O.M, et al., 2023. Comparative effects of curcumin versus nano-curcumin on histological, immunohistochemical expression, histomorphometric, and biochemical changes to pancreatic beta cells and lipid profile of streptozocin induced diabetes in male Sprague-Dawley rats. Environmental Science and Pollution Research. Ahead of Print. 10.1007/s11356-023-26260-6